Molecular Cell
Article

Gcn5 Promotes Acetylation, Eviction, and Methylation of Nucleosomes in Transcribed Coding Regions

Chhabi K. Govind,[1] Fan Zhang,[1] Hongfang Qiu,[1] Kimberly Hofmeyer,[1] and Alan G. Hinnebusch[1,*]
[1] Laboratory of Gene Regulation and Development, National Institute of Child Health and Human Development, Bethesda, MD 20892, USA
*Correspondence: ahinnebusch@nih.gov
DOI 10.1016/j.molcel.2006.11.020

SUMMARY

We report that coactivator SAGA, containing the HAT Gcn5p, occupies the *GAL1* and *ARG1* coding sequences during transcriptional induction, dependent on PIC assembly and Ser5 phosphorylation of the Pol II CTD. Induction of *GAL1* increases H3 acetylation per nucleosome in the ORF, dependent on SAGA integrity but not the alternative Gcn5p-HAT complex ADA. Unexpectedly, H3 acetylation in *ARG1* coding sequences does not increase during induction due to the opposing activities of multiple HDAs associated with the ORF. Remarkably, inactivation of Gcn5p decreases nucleosome eviction from both *GAL1* and a long (∼8 kb) ORF transcribed from the *GAL1* promoter. This is associated with reduced Pol II occupancy at the 3′ end and decreased mRNA production, selectively, for the long ORF. Gcn5p also enhances H3-K4 trimethylation in the *ARG1* ORF and bulk histones. Thus, Gcn5p, most likely in SAGA, stimulates modification and eviction of nucleosomes in transcribed coding sequences and promotes Pol II elongation.

INTRODUCTION

SAGA is a transcriptional coactivator in budding yeast that is recruited by activators to the upstream activation sequences (UASs) of yeast promoters (Bhaumik and Green, 2001; Cosma et al., 1999; Larschan and Winston, 2001; Swanson et al., 2003). SAGA contains the histone acetyltransferase (HAT) Gcn5p, which modifies Lys residues 9 and 14 (among others) in histone H3. Histone acetylation by Gcn5p has been implicated in displacement of promoter nucleosomes during transcriptional activation (Barbaric et al., 2001; Filetici et al., 1998) and in aiding recruitment of TBP, RNA Polymerase II (Pol II) (Qiu et al., 2004), and coactivators (Geng and Laurent, 2004; Govind et al., 2005) to yeast promoter regions. Other SAGA subunits enhance preinitiation complex (PIC) assembly by a mechanism that goes beyond the HAT activity of the complex (Bhaumik and Green, 2001; Govind et al., 2005; Larschan and Winston, 2001; Qiu et al., 2004).

It appears that SAGA also stimulates the elongation phase of transcription. Histones in coding regions, in addition to promoters, show high basal acetylation in yeast, and severe hypoacetylation from simultaneously inactivating Gcn5p and the HAT Elp3 reduces transcription more so than PIC assembly at many genes (Kristjuhan et al., 2002). We found previously that deleting *GCN5* or *ADA1* (the latter disrupting SAGA) reduced Pol II occupancy more severely in coding sequences than in the promoter of *ARG1*, suggesting an elongation defect (Govind et al., 2005). Genetic and physical interactions between SAGA subunit Spt8p and elongation factor TFIIS (Dst1p) have also been described (Milgrom et al., 2005; Wery et al., 2004). However, there are indications that SAGA is restricted largely to the UAS elements at transcribed genes (Larschan and Winston, 2001; Robert et al., 2004), suggesting that its potential roles in elongation could be indirect.

We report here that SAGA is associated at high levels with the coding sequences of *GAL1* and of genes induced by activator Gcn4p and that SAGA occupancy of the ORF requires transcription and phosphorylation of Ser5 in the C-terminal domain (CTD) of Pol II subunit Rpb1p. We show also that Gcn5p, most likely in SAGA, performs several important functions in transcribed coding sequences. It increases histone H3 acetylation, enhances nucleosome eviction from the highly transcribed *GAL1* gene, and promotes Pol II processivity to an extent that elevates transcriptional output from an extended ORF. Gcn5p also increases the efficiency of trimethylation of H3-Lysine 4 in transcribed coding sequences.

RESULTS

Transcription-Dependent Targeting of SAGA to Coding Regions Is Stimulated by CTD-Ser5 Phosphorylation by Kin28p

To explore functions of SAGA in elongation, we asked whether SAGA is recruited by activators to the coding sequences of their target genes. Chromatin immunoprecipitation (ChIP) analysis revealed the expected increase

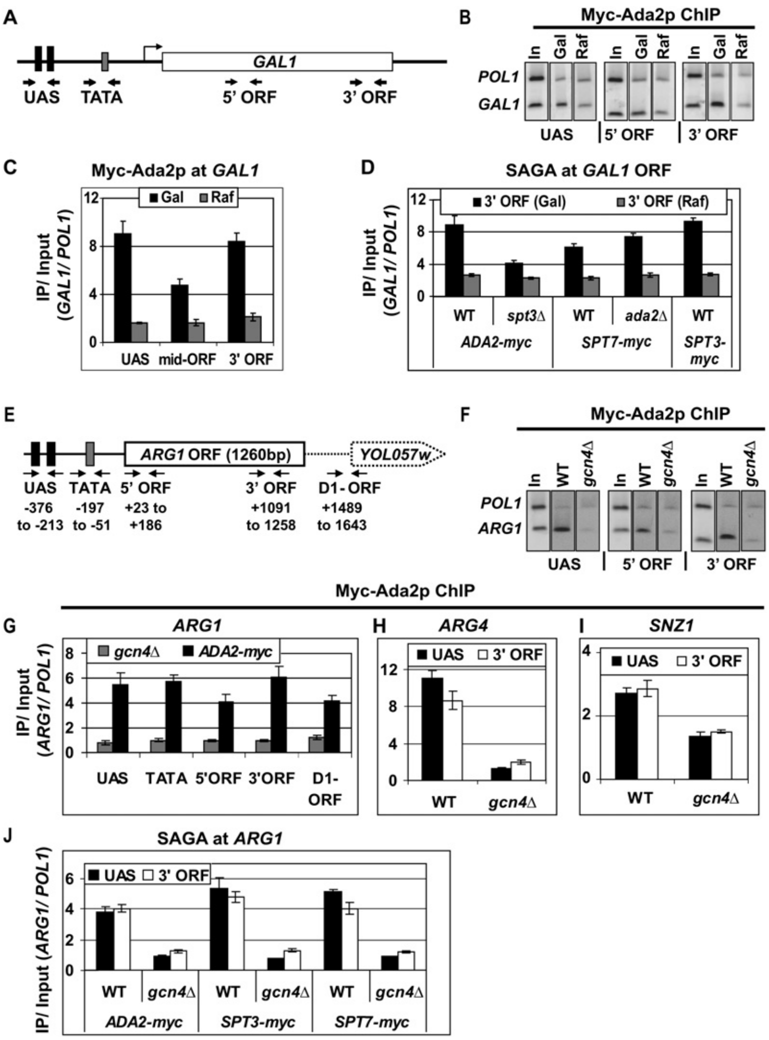

Figure 1. SAGA Is Targeted to Coding Sequences

(A) *GAL1* showing primers used for ChIP analysis. Forward primers for 5′ and 3′ ORF sequences are at 422 and 1233 bp, respectively, from the beginning of the ORF.

(B) Representative ChIP data for Myc-Ada2p occupancy at *GAL1*. *ADA2-myc* strain HQY392 was grown at 30°C in yeast peptone medium containing 2% raffinose (YP_{Raf}) (Raf) and induced with 2% Galactose (Gal) for 30 min. ChIP was performed with anti-Myc antibodies and primers to amplify *GAL1* UAS, 5′ ORF, and 3′ ORF sequences (or the *POL1* ORF as a reference sequence), from DNA purified from immunoprecipitated or input (In) chromatin samples.

(C) The ratio of IP to input signals was calculated for *GAL1* and divided by the corresponding ratio for the reference sequence (*POL1* ORF), and the mean and standard errors of the resulting normalized IP/Input ratios from replicate cultures, calculated with three PCR measurements, are plotted.

(D) Analysis as in (C) with the relevant strains listed in Table S1.

(E) *ARG1* showing primers for ChIP analysis and their locations relative to the beginning of the ORF.

(F) Representative data for Myc-Ada2p occupancy at *ARG1*. *ADA2-myc GCN4* (HQY392) and *ADA2-myc gcn4Δ* (HQY503) cells growing at 30°C in SC medium lacking Ile and Val (SC-Ile/Val) were treated with 0.6 μM sulfometuron (SM) for 30 min and subjected to ChIP analysis with anti-Myc antibodies and the *ARG1* primers shown in (E).

(G–I) Summary of ChIP data from HQY392 and HQY503 using the indicated primers from *ARG1*, *ARG4*, or *SNZ1* (Table S2).

(J) Analysis as in (G).

All error bars represent the standard errors of the mean (SEM).

in association of myc-tagged SAGA subunit Ada2p with the *GAL1* UAS element in cells grown with galactose (inducing) versus raffinose (noninducing) as carbon source. Surprisingly, Myc-Ada2p and two other tagged SAGA subunits, Myc-Spt7p and Myc-Spt3p, were also associated with sequences in the 5′ or 3′ ends of the *GAL1* ORF under inducing conditions (Figures 1A–1D). Deletion of *SPT3* reduced Myc-Ada2p occupancy, whereas deleting *ADA2* had no effect on Myc-Spt7p occupancy of the ORF (Figure 1D), consistent with the subunit requirements for SAGA recruitment to a UAS (Qiu et al., 2005). Binding of activator Gal4p was confined to the UAS under inducing conditions (see Figure S1A in the Supplemental Data available with this article online). These data demonstrate that SAGA is targeted to the *GAL1* ORF during transcriptional induction.

We found that SAGA is also targeted to coding regions of genes induced by activator Gcn4p in amino-acid-limited cells where Gcn4p binding to UAS elements is induced (Govind et al., 2005). We observed high-level Gcn4p-dependent association of Myc-Ada2p with the UAS, the promoter, 5′ and 3′ ends of the ORF, and sequences downstream of the ORF at *ARG1* (Figures 1E–1G), and at the UAS and 3′ ORF sequences at *ARG4* and *SNZ1* (Figures 1H and 1I). We also saw Gcn4p-dependent binding of Myc-Spt3p and Myc-Spt7p at UAS and ORF sequences at *ARG1* (Figure 1J). Binding of Gcn4p, mediator, and SWI/SNF was confined to the UAS elements (Figures S1B and S1C). Thus, two different yeast activators can target SAGA to transcribed coding sequences.

Promoter and terminator regions can be found physically associated in yeast cells (O'Sullivan et al., 2004) dependent on transcription and the Pol II CTD phosphatase SSU72, and it was proposed that "gene looping" facilitates transcription reinitiation (Ansari and Hampsey, 2005). If gene looping was responsible for SAGA occupancy in the *ARG1* ORF, then TBP and TFIIB should also be associated with 3′ ORF sequences at nearly the same high levels observed at the promoter. However, we observed low occupancies for both factors at the *ARG1* 3′

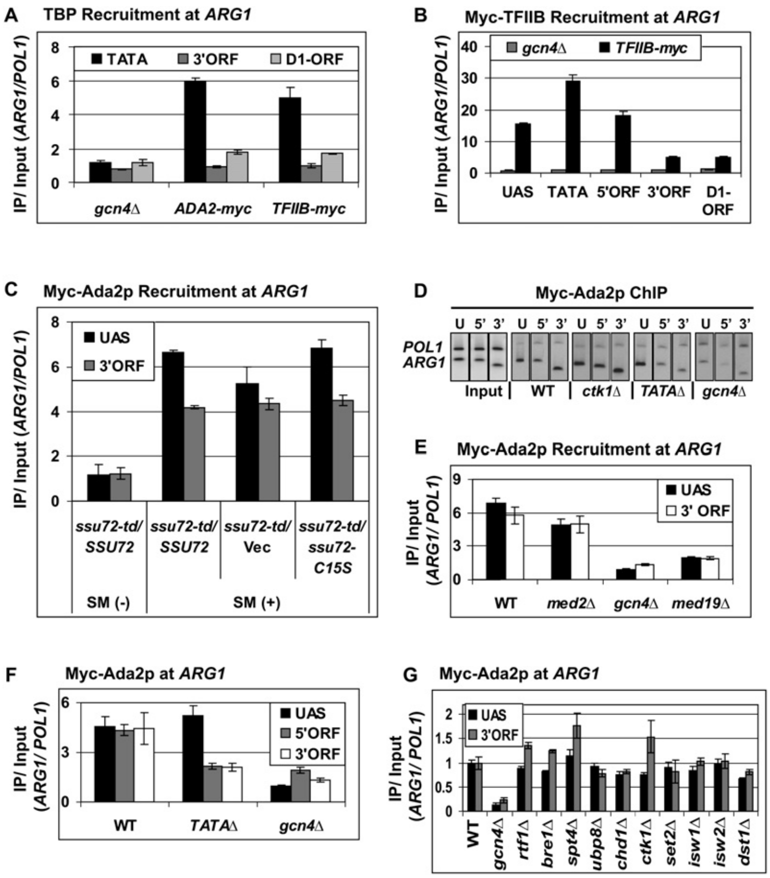

Figure 2. Targeting SAGA to the *ARG1* ORF Requires PIC Assembly but Is Independent of Ssu72p

(A and B) TFIIB and TBP occupancy is restricted to the promoter. *ADA2-myc* and *SUA7-myc* strains were cultured and subjected to ChIP analysis of TBP (A) or Myc-TFIIB/SUA7 (B) occupancy at *ARG1* as described in Figure 1F except using TBP antibodies in (A).

(C) Inactivation of Ssu72p does not affect SAGA occupancy at *ARG1*. *ADA2-myc* tagged strains bearing the *ssu72-td* degron allele and plasmid-borne WT *SSU72* or *ssu72-C15S*, or empty vector (Vec), were grown at 25°C to A_{600} of 0.5, transferred to 37°C for 30 min, and induced with SM (0.6 μM) for 30 min at 37°C (SM[+]), or left untreated with SM (SM[−]). ChIP was conducted with anti-Myc antibodies.

(D–G) Cofactor requirements for SAGA association with the *ARG1* ORF. *ADA2-myc* strains were cultured and subjected to ChIP analysis of Myc-Ada2p occupancy at *ARG1* as in Figure 1F.

(G) Results for mutant strains were normalized to those for WT.

All error bars represent the SEM.

end (cf. Figure 1G and Figures 2A and 2B). Additionally, depletion of SSU72 in a degron mutant (*ssu72-td*) or a point mutation that impairs its phosphatase activity (*ssu72-C15S*), both of which diminish gene looping in the strains we analyzed (Krishnamurthy et al., 2004), had no effect on the 3′ ORF occupancy of SAGA at *ARG1* (Figure 2C). As expected (Krishnamurthy et al., 2004), both *ssu72* mutants show elevated Ser5 phosphorylation of the Pol II CTD at the 3′ end of *ARG1* (Figure S4 and data not shown). Thus, gene looping is not responsible for high-level association of SAGA with the *ARG1* ORF.

We hypothesized that recruitment of SAGA to the UAS is needed for its subsequent spreading into the *ARG1* ORF. Mediator promotes SAGA recruitment by Gcn4p at the UAS, and deleting the *ROX3/MED19* and *MED2* Mediator subunits produces strong and modest reductions, respectively, in SAGA recruitment to the *ARG1* UAS (Govind et al., 2005; Qiu et al., 2005). Consistent with our hypothesis, *med19Δ* and *med2Δ* mutations reduced SAGA occupancy in the *ARG1* ORF commensurate with their effects on UAS occupancy (Figure 2E). Because Mediator mutations reduce *ARG1* transcription, diminished SAGA occupancy might result from decreased Pol II density in the ORF. Supporting this interpretation, deletion of the *ARG1* TATA element, which reduces Pol II occupancy in the ORF and mRNA production (Qiu et al., 2006), decreased SAGA occupancy in the ORF but not the UAS (Figures 2D and 2F). The data suggest that association of SAGA with the coding sequences depends on PIC assembly and transcription.

Previous findings suggested that SAGA recruitment to the *GAL1* UAS might be stimulated by interaction of subunit Chd1p with histone H3 methylated on Lys4 (H3-K4) (Pray-Grant et al., 2005). Thus, SAGA recruitment to the *ARG1* ORF could require Chd1p and factors implicated in H3-K4 trimethylation, including H2B ubiquitinating factor *BRE1*, the *RTF1* subunit of Paf1 complex (Sims et al., 2004), the deubiquitinase *UBP8* (Daniel et al., 2004), and elongation factor *SPT4* (Qiu et al., 2006). However, deletions of these genes produced only small or no reductions in Gcn4p-dependent SAGA occupancy of the *ARG1* UAS or ORF sequences (Figure 2G). Similar results were obtained for deletion of H3-K36 methylase *SET2*, Pol II CTD-Ser2 kinase *CTK1*, and the *ISW1* and *ISW2* subunits of nucleosome remodeling factors, all implicated previously in modifications of ORF nucleosomes (Sims et al., 2004; Zhang and Reese, 2004). The *dst1Δ* mutant lacking TFIIS also displayed only a small decrease in SAGA occupancy of ORF sequences (Figure 2G). Thus, none of the elongation factors we examined plays a critical role in SAGA association with the *ARG1* ORF.

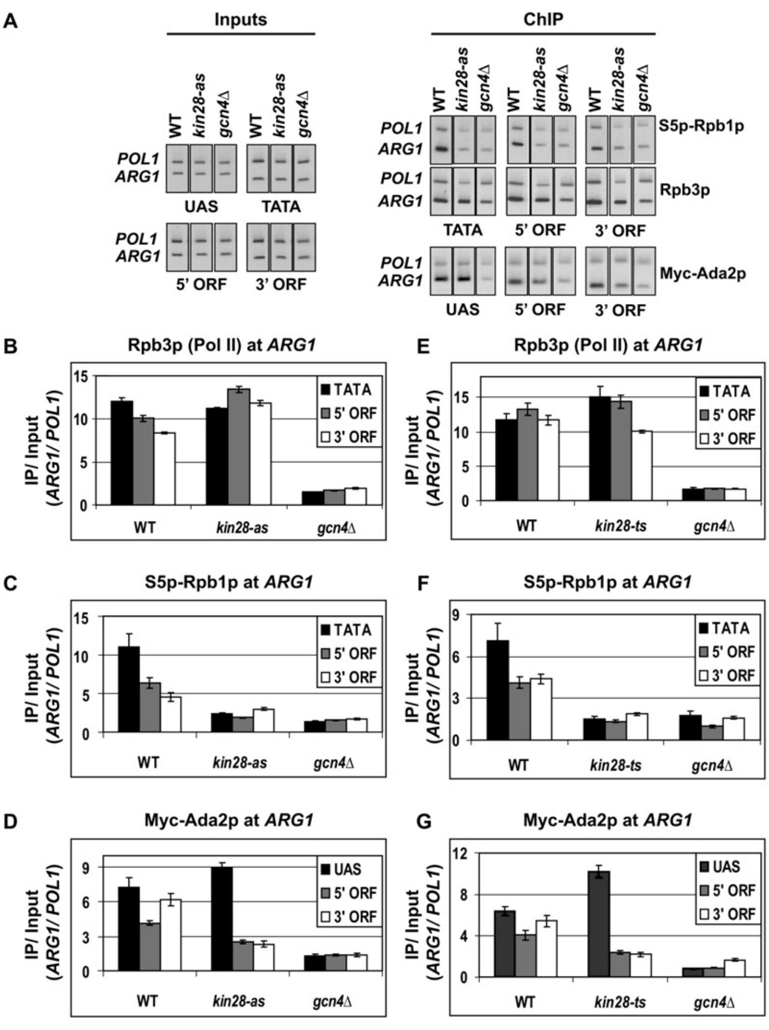

Figure 3. SAGA Targeting to the *ARG1* ORF Requires Kin28p-Dependent CTD Phosphorylation

(A–D) *ADA2-myc KIN28* (CGY110), *ADA2-myc kin28-as* (CGY112), and *ADA2-myc gcn4Δ* (HQY503) cells were cultured in SC-Ile/Val at 30°C, treated with 12 μM of NA-PP1 for 12 min, and induced with SM for 30 min. ChIP analysis was performed as in Figure 1F to measure occupancy of Myc-Ada2p, Rpb1p-CTD phosphorylated on Ser5 (S5p-Rpb1p), and Rpb3p at *ARG1*.

(E–G) *ADA2-myc KIN28-HA* (CGY88), *ADA2-myc kin28-HA-ts16* (CGY86), and *ADA2-myc gcn4Δ* (CGY80) cells were cultured in SC-Ile/Val at 25°C, transferred to 37°C for 30 min, and treated with SM for another 30 min at 37°C, then subjected to ChIP analysis as in (B)–(D).

All error bars represent the SEM.

Considering that association of mRNA processing factors with elongating Pol II is stimulated by Ser5 phosphorylation of the CTD (Sims et al., 2004), we asked whether impairment of CTD-Ser5 kinase Kin28p would diminish SAGA occupancy in the ORF. *kin28-as* (analog-sensitive) mutant cells were treated with NA-PP1 to inhibit Kin28p kinase activity, after which Gcn4p was induced by amino acid limitation in the presence of NA-PP1. In wild-type cells, Pol II phosphorylated on Ser5 (S5p-Pol II) occurs at the highest level in the promoter and lowest level at the 3′ end of *ARG1* (compare S5p-Rpb1p and Rpb3p in WT in Figures 3B and 3C). As expected (Qiu et al., 2006), inhibition of the *kin28-as* product reduces S5p-Pol II across the gene without decreasing Pol II occupancy, producing Ser5-hypophosphorylated Pol II at *ARG1* (Figures 3B and 3C). Importantly, Myc-Ada2p occupancy was reduced in the *kin28-as* cells at the 5′ and 3′ ends of the ORF, but not in the UAS (Figure 3D). Similar results were obtained using a temperature-sensitive *kin28-ts16* mutant (Figures 3E–3G). We conclude that Ser5-hyperphosphorylation of Pol II promotes SAGA occupancy in the *ARG1* ORF.

Evidence that SAGA Mediates H3 Acetylation of ORF Nucleosomes during Transcription

Gcn5p contributes to H3 acetylation of promoter and ORF nucleosomes at constitutively transcribed or even repressed genes (Kristjuhan et al., 2002; Kuo et al., 2000; Vogelauer et al., 2000), and it mediates targeted acetylation in promoters during transcriptional activation (Krebs et al., 2000, 1999; Kuo et al., 2000; Reinke and Horz, 2003) as a subunit of SAGA (Dudley et al., 1999). Having found that SAGA is targeted to the ORF, we asked whether it functions in transcription-coupled H3 acetylation of coding sequences by Gcn5p.

H3 diacetylated on K9 and K14 (henceforth H3Ac) in bulk chromatin is greatly reduced in our *gcn5Δ* strain in a manner complemented by *GCN5* (Figure 4A). Moreover, ChIP analysis of constitutively transcribed genes *PMA1* and *PYK1* revealed higher levels of H3Ac in the TATA and 5′ ORF sequences versus nontranscribed sequences at the telomere VI right arm (*TEL*), and *gcn5Δ* greatly reduced H3Ac levels at the *PMA1*, *PYK1*, and *TEL* loci (Figures S2A and S2B). Thus, our data confirm that Gcn5p makes a large contribution to H3 acetylation of promoter

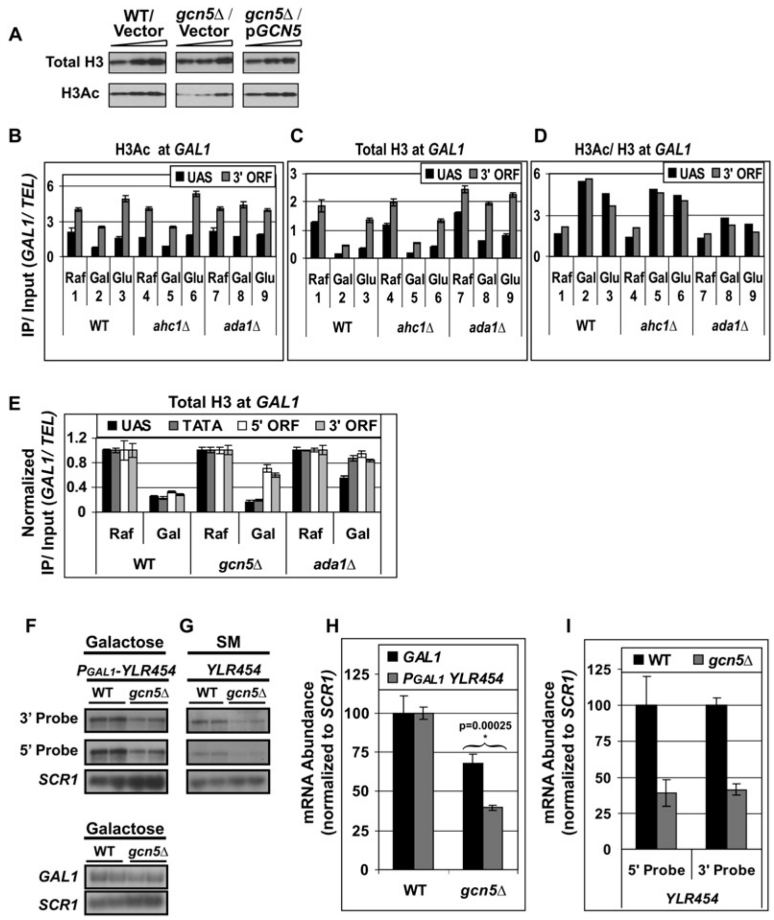

Figure 4. Involvement of Gcn5p and SAGA in H3 Acetylation of *GAL1* Coding Sequences

(A) *GCN5* strain HQY392 bearing empty vector and *gcn5Δ* strain CGY99 containing vector or *GCN5* plasmid pRS316-GCN5 were grown in SC lacking uracil (SC-Ura), and whole-cell extracts (WCEs) were subjected to western blot analysis with antibodies against total histone H3 or H3 diacetylated on K9 and K14 (H3Ac). The panels shown derive from the same western blots.

(B–D) Wild-type (HQY392), *gcn5Δ* (CGY99), *ahc1Δ* (1799), and *ada1Δ* (HQY418) strains were grown in SC_{Raf}, induced with 2% galactose for 2.5 hr, and repressed with 4% glucose for 4 min. ChIP analysis of H3Ac and total H3 in the *GAL1* UAS, 5′ ORF, or 3′ ORF and of the reference *TEL* sequence was conducted as described in Figure 1. (B)–(D) summarize the data obtained for H3Ac occupancy (B), total H3 (C), and the H3Ac to total H3 ratio (D), respectively, for WT, *ahc1Δ*, and *ada1Δ* strains.

(E) Total H3 occupancy at *GAL1* in WT, *gcn5Δ*, and *ada1Δ* cells, with occupancies in galactose normalized to those in raffinose.

(F) Northern analysis of duplicate cultures of *GCN5* P_{GAL1}-*YLR454* (CGY101) and *gcn5Δ* P_{GAL1}-*YLR454* (CGY122) strains grown in SC_{Raf} at 30°C and induced with 2% galactose for 30 min, probing with [^{32}P]-labeled DNA fragments from the 5′ (0.5 kb–2 kb) or 3′ end (6–8 kb) of *YLR454* (upper panels), *GAL1* (+422 to +1355 bp) (lower panels), and *SCR1* (loading control).

(G) Northern analysis of native *YLR454* in WT (HQY392) and *gcn5Δ* (CGY99) strains grown in the presence of SM.

(H) Mean *GAL1/SCR1* and P_{GAL1}-*YLR454/SCR1* transcript ratios measured by phosphorimaging analysis from replicates of the experiment in (F) are plotted for *GCN5* and *gcn5Δ* strains, with WT levels set to 100%. The p value of a t test (two-tailed distribution with unequal variance) for the difference between *GAL1* and P_{GAL1}-*YLR454* mRNA in *gcn5Δ* cells is indicated (*).

(I) Analysis of northern data from multiple replicates of the experiment in (G).

All error bars represent the SEM.

and coding sequences of constitutively transcribed genes and in chromatin at large.

We asked next whether Gcn5p participates in transcription-coupled H3 acetylation during induction of *GAL1* and whether it functions in the context of SAGA or the alternative Gcn5p-containing complex ADA. After 30 min of galactose induction, we saw a decrease, rather than increase, in the absolute levels of H3Ac at both the UAS and 3′ ORF sequences in WT cells (Figure 4B, lanes 1 and 2). However, galactose induction produced a marked depletion of total H3 in the *GAL1* UAS and ORF (Figure 4C, lanes 1 and 2), as shown for the coregulated genes *GAL10* and *GAL7* (Schwabish and Struhl, 2004) and for *PHO5* (Reinke and Horz, 2003). After correcting for histone eviction, there was a net increase in H3Ac per nucleosome (H3Ac/H3 ratio) in both UAS and ORF (Figure 4D, lanes 1 and 2). Thus, transcriptional induction elicits increased acetylation of the histone H3 that remains in both promoter and coding sequences at *GAL1*. Deletion of *GCN5* reduced H3Ac in the UAS and ORF sequences after 30 min of galactose induction without lowering the total H3 level (Figure S2C), showing that Gcn5p is a major contributor to H3 acetylation of ORF and UAS sequences during high-level transcription of *GAL1*.

The ADA complex shares Gcn5p with SAGA but contains Ahc1p as a unique constituent and lacks many subunits found in SAGA, including Ada1p (Eberharter et al., 1999). Disrupting ADA by the *ahc1Δ* mutation had little effect on absolute levels of H3Ac, total H3, or the H3Ac/H3 ratio under inducing conditions (Figures 4B–4D, lanes 2 and 5). By contrast, disrupting SAGA by *ada1Δ* substantially reduced the H3Ac/H3 ratio in the *GAL1* ORF and UAS under inducing conditions (Figure 4D, lanes 2 and 8). The absolute levels of H3Ac in UAS and ORF were actually higher in *ada1Δ* compared to WT cells under inducing conditions (Figure 4B, lanes 2 and 8), but *ada1Δ* reduces histone eviction from the UAS and completely eliminates histone loss from the ORF (Figure 4C, lanes 2 and 8) to yield a net decrease in H3Ac/H3 ratios for UAS and ORF sequences. These results are consistent with a role for SAGA, but not ADA complex, in transcription-coupled H3 acetylation of the induced *GAL1* ORF. However, because deletion of *ADA1* impairs transcriptional induction of *GAL1* (Bhaumik and Green, 2001, 2002; Dudley et al., 1999), it is possible that *ada1Δ* reduces H3 acetylation indirectly by impeding an unknown Gcn5p-containing complex that would occupy transcribed coding sequences in the manner described here for SAGA.

We investigated next whether the restoration of nucleosomes that occurs following glucose-repression of *GAL1* transcription is accompanied by H3 acetylation, as this function could be carried out by SAGA molecules that occupy the ORF during transcriptional induction. By 4 min after addition of glucose, total H3 levels increased above their levels in inducing conditions (Figure 4C, lanes 2 and 3), consistent with reassembly of nucleosomes in the UAS and ORF on cessation of PIC assembly and transcription. Importantly, the level of H3Ac also increased with glucose addition (Figure 4B, lanes 2 and 3), resulting in a higher H3Ac/H3 ratio than in noninducing (raffinose) conditions (Figure 4D, lanes 1 and 3). The *ahc1Δ* mutation had little effect on recovery of total H3 or its acetylation on glucose addition (Figures 4B–4D, lanes 2 and 3 versus 5 and 6). In *ada1Δ* cells, there is little change in total H3 or H3Ac levels on glucose repression (Figures 4B–4D, lanes 8 and 9). This was expected because transcriptional induction by galactose is strongly impaired in this mutant. The fact that H3 acetylation of reassembled ORF nucleosomes occurred in the absence of ADA complex is consistent with the idea that SAGA targeted to the coding sequences during transcription carries out this function. However, the possibility of nucleosome reassembly in the ORF from a pool of preacetylated histones cannot be ruled out. It could also be proposed that chromatin is reassembled using the same acetylated nucleosomes that were evicted during transcription. This last possibility seems unlikely in view of recent findings that new histones are readily incorporated in *trans* behind transcribing RNA polymerases (Linger and Tyler, 2006; Schermer et al., 2005).

Gcn5p Is Required for Optimal Nucleosome Eviction from Highly Transcribed ORF Sequences

As shown above, deletion of *ADA1* nearly eliminates depletion of nucleosomes in the ORF and dampens nucleosome loss in the UAS during *GAL1* induction (Figure 4C, lanes 1 and 2 versus 7 and 8). Interestingly, *gcn5Δ* differs from *ada1Δ* in having no effect on H3 loss in the UAS but resembles *ada1Δ* in reducing H3 eviction from the ORF during induction (Figure 4E). These findings suggest that H3 acetylation by Gcn5p is required for optimal nucleosome eviction in the ORF, whereas a non-HAT SAGA function promotes nucleosome loss in the promoter. Unlike *ada1Δ*, the *gcn5Δ* mutation has little effect on Pol II density in the ORF during induction (data not shown) and reduces *GAL1* mRNA levels by only ~30% (Figures 4F [lower panel] and 4H). Hence, the defect in nucleosome eviction in *gcn5Δ* cells is probably not a secondary effect of reduced transcription.

We sought additional evidence that Gcn5p promotes nucleosome eviction from coding sequences and wished to determine whether a defect in this activity might impair elongation. If so, it could have a more pronounced effect on transcription of an ORF much longer than *GAL1*. Toward this end, we conducted kinetic ChIP analysis of the 8-kb-long ORF of *YLR454* placed under control of the *GAL1* promoter (P_{GAL1}-*YLR454*). As expected (Mason and Struhl, 2005), following addition of glucose, Pol II was lost from the promoter within ~1.5 min, from the middle of the ORF within ~3 min, and from the 3′ end of the ORF within ~5 min, reflecting run-off of elongating Pol II molecules present at the time of glucose addition (Figure 5A, bottom part of the graph). Importantly, disappearance of Pol II was mirrored by an increase in H3Ac and total H3 at each location, so that H3Ac per nucleosome remained nearly constant during reassembly of nucleosomes after passage of Pol II (Figures 5A–5C, upper parts of graphs). These findings support the idea that nucleosomes newly deposited in the wake of elongating Pol II are rapidly acetylated to the level that occurs during induction.

In *gcn5Δ* cells, Pol II run-off was not accompanied by an increase in H3 acetylation across the P_{GAL1}-*YLR454* ORF (Figure 5D, upper part of graph), in accordance with the prominent role played by Gcn5p in H3 acetylation of coding sequences. Total H3 levels also increased very little on glucose repression in *gcn5Δ* cells (Figures 5E and 5G), which may stem partly from the fact that H3 levels do not decline much in the first place during galactose induction in *gcn5Δ* cells (Figure 5G). This last observation supports the finding above that H3 eviction from the authentic *GAL1* ORF is diminished by *gcn5Δ* (Figure 4E). Together, these data suggest that H3 acetylation by Gcn5p promotes eviction of ORF nucleosomes during high-level transcription.

The *gcn5Δ* mutation had no obvious effect on the rate of Pol II run-off in the P_{GAL1}-*YLR454* ORF (cf. Figures 5A and 5D, lower parts of graphs), suggesting that the higher nucleosome density in *gcn5Δ* cells does not reduce the transcription elongation rate. Similarly, the *asf1Δ* mutation reduces the extent of H3 eviction during transcription of the P_{GAL1}-*YLR454* ORF but does not lower the rate of Pol II elongation (Schwabish and Struhl, 2006). However, we did observe a progressive decline in Pol II occupancy across the P_{GAL1}-*YLR454* ORF under inducing conditions in *gcn5Δ* cells (Figure 5H), suggesting reduced Pol II processivity in the absence of Gcn5p. The fact that Pol II loss is detectable only at distances of 4 kb or greater from the promoter can explain why it was not observed for the (~1.6 kb) *GAL1* ORF.

Importantly, *gcn5Δ* conferred a larger reduction in mRNA from the P_{GAL1}-*YLR454* gene than from native *GAL1* (reduction of 60% versus 30%, p = .00025; Figures 4F and 4H), and it reduced mRNA from P_{GAL1}-*YLR454* and native *YLR454* by nearly identical amounts (Figures 4F and

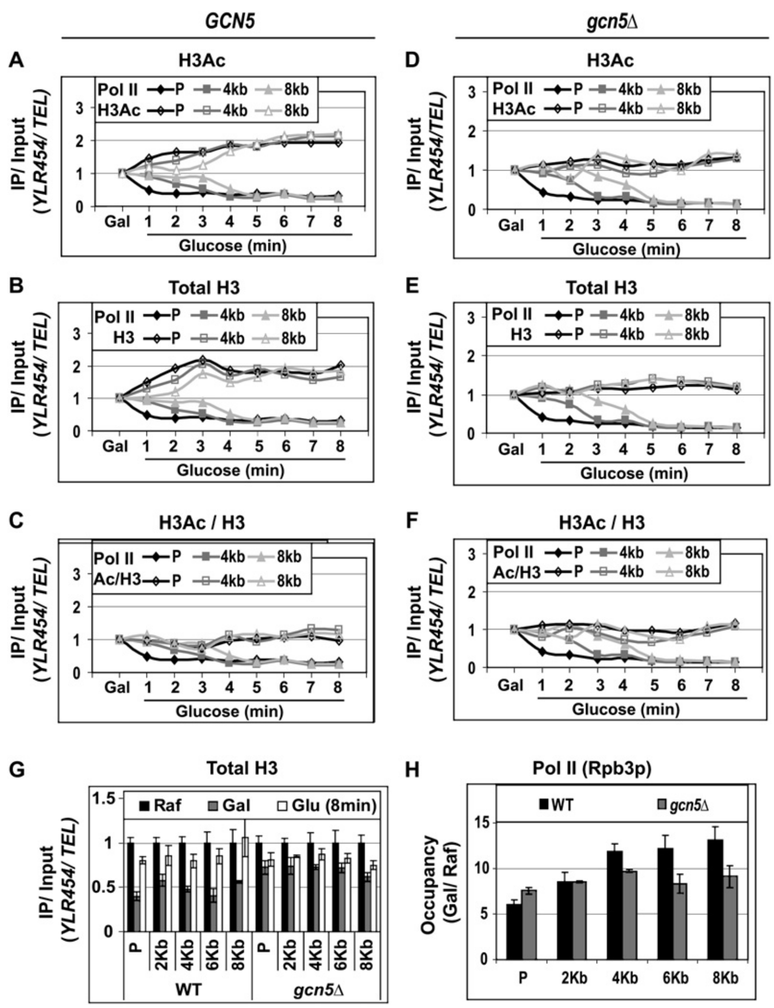

Figure 5. Involvement of Gcn5p in H3 Acetylation of Nucleosomes Reassembled after Repression of *P_{GAL1}-YLR454* Transcription

GCN5 P_{GAL1}-YLR454 (CGY101) and *gcn5Δ P_{GAL1}-YLR454* (CGY122) strains were grown in SC_{Raf}, induced with 2% galactose for 2.5 hr, and repressed with 4% glucose. Aliquots collected every min, up to 8 min, in glucose were subjected to ChIP analysis of Rpb3p, H3Ac, and total H3 occupancy in the promoter and at 2 kb intervals across the *P_{GAL1}-YLR454* ORF.

(A–C) Comparison of Pol II (Rpb3p) occupancy (filled symbols) with that of H3Ac (A), total H3 (B), and the H3Ac/H3 ratio (C) (open symbols) in the promoter (P) and at 4 kb or 8 kb distances into the ORF, in WT cells induced with galactose and repressed by glucose for increasing times.

(D–F) Same as (A)–(C) for *gcn5Δ* cells. The occupancies of all factors in glucose are presented relative to those in galactose. The standard error of the mean (SEM) for each point was <20% (data not shown).

(G) Comparison of total H3 occupancy in the WT and *gcn5Δ* strains in cells grown with raffinose, induced with galactose, or repressed with glucose for 8 min. The H3 occupancy at each location in galactose or glucose (8 min) was expressed relative to that in raffinose (set to unity).

(H) Comparison of Pol II (Rpb3p) occupancy at different locations following galactose induction in WT and *gcn5Δ* cells, expressed as the ratio of occupancies in galactose versus raffinose medium.

All error bars represent the SEM.

4G). Considering that *P_{GAL1}-YLR454* and *GAL1* have the same promoter, and our finding that *gcn5Δ* does not impair Pol II occupancy at the *P_{GAL1}-YLR454* promoter (Figure 5H), the larger reduction in mRNA from *P_{GAL1}-YLR454* versus *GAL1* in *gcn5Δ* cells provides additional evidence for a defect in Pol II processivity, which has greater consequences for a long ORF than for a short one.

H3 Acetylation in the Induced *ARG1* ORF Reflects a Balance between Gcn5p and Multiple Histone Deacetylases

We extended our analysis of Gcn5p-dependent acetylation of coding sequences to the Gcn4p-induced gene *ARG1*. The levels of H3Ac at the UAS, TATA region, and ORF sequences were greatly reduced in *gcn5Δ* cells under inducing conditions (Figure 6A), implicating Gcn5p in H3 acetylation at *ARG1*. Similar to *GAL1*, induction of *ARG1* led to decreased, rather than increased, absolute levels of H3Ac at UAS and TATA sequences [Figure 6B, UAS and TATA, WT(UI) versus WT(I)], and as expected, this decline in H3 acetylation required Gcn4p (Figure 6A, *gcn4*(I) versus WT(I)). Because of even greater Gcn4p-dependent loss of H3 in the UAS and TATA (Figure 6C), the H3Ac per nucleosome in the promoter increased during induction by Gcn4p (Figure 6D). This increase in H3Ac per nucleosome also depends partly on SAGA integrity (Ada1p) and the TATA element but not on Ahc1p (Figure 6E, UAS, TATA). These data indicate that Gcn5p acetylates promoter nucleosomes in the context of SAGA. (Our findings differ from previous results for Gcn4p target genes *HIS3* and *TRP3*, for which absolute levels of H3Ac increased on Gcn4p induction [Deckert and Struhl, 2001; Kuo et al., 2000]. However, because total H3 levels were not analyzed in these studies, the increases in acetylation per nucleosome could be comparable at the different Gcn4p target genes that have been studied.)

When we examined *ARG1* ORF sequences, we saw a decrease in the absolute level of H3Ac on induction by Gcn4p (Figure 6B, 5′ ORF and 3′ ORF), and as total H3 levels were reduced by a similar or smaller amount (Figure 6C), there was no net change (5′ ORF) or a decrease (3′ ORF) in acetylation per nucleosome under inducing conditions (Figure 6D). As expected, the

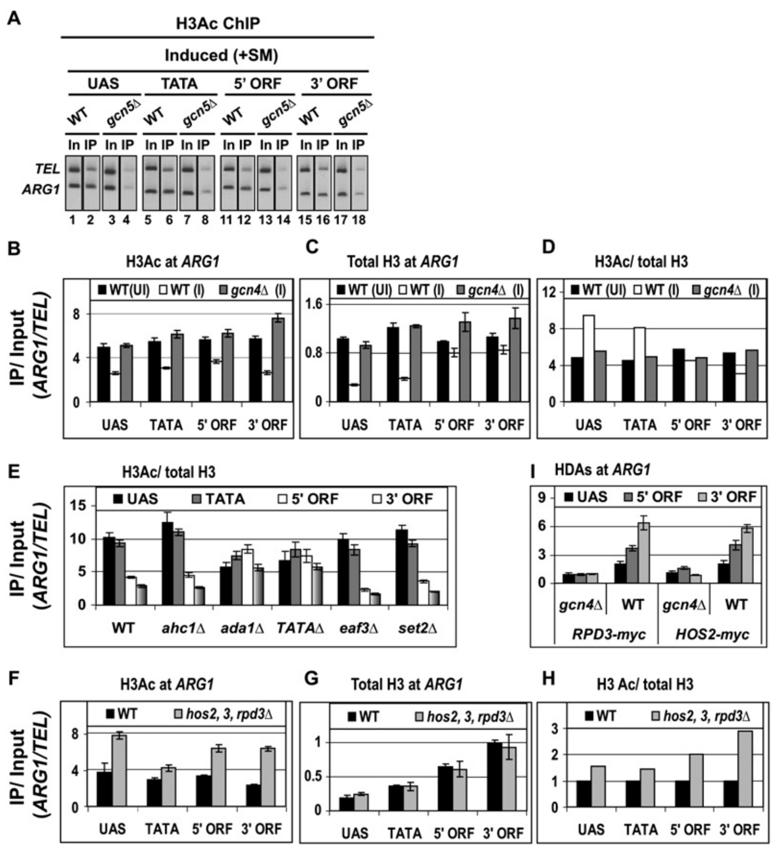

Figure 6. Opposing Activities of Gcn5p and Multiple HDAs in Acetylation of *ARG1* Coding Sequences

(A–H) The WT and indicated mutant strains were grown in SC-Ile/Val and treated with SM to induce Gcn4p and subjected to ChIP analysis to measure occupancies of H3Ac and total H3 at *ARG1*. (A) shows representative H3Ac ChIP data for the WT (HQY392) and *gcn5Δ* (CGY99) strains under inducing conditions. (B)–(D) compare the occupancies of H3Ac (B), total H3 (C), and the H3Ac/H3 ratio (D) in WT (HQY392) and *gcn4Δ* (HQY503) strains in uninducing (UI) and inducing (I) conditions. (E) compares the ratio of H3Ac to total H3 occupancies between WT (HQY392) and mutant strains 1799 (*ahc1Δ*), HQY418 (*ada1Δ*), CGY51 (*TATAΔ*), 7143 (*eaf3Δ*), and CGY90 (*set2Δ*). (F)–(H) compare the occupancies of H3Ac (F), total H3 (G), and the H3Ac/H3 ratio (H) in WT (DY151) and *hos2Δ hos3 rpd3Δ* (DY4565) strains under inducing conditions.

(I) Occupancies of Myc-Rpd3p and Myc-Hos2p at *ARG1* (UAS and ORF) in WT and *gcn4Δ* cells, measured by ChIP as in Figure 1.

All error bars represent the SEM.

decreases in absolute levels of H3Ac and total H3 in the 3′ ORF did not occur in *gcn4Δ* cells (Figures 6B–6D), and the *ada1Δ* and Δ*TATA* mutations likewise produced higher, not lower, acetylation per nucleosome in both 5′ and 3′ ORF sequences (Figure 6E, 5′ and 3′ ORF). Together, these data suggest that induction of *ARG1* by Gcn4p leads to decreased acetylation per nucleosome in the ORF. How can we reconcile this conclusion with our finding that SAGA associates with the *ARG1* coding sequences during transcriptional induction by Gcn4p (Figures 1F and 1G)?

One possibility is that recruitment of the histone deacetylase (HDA) Rpd3p to *ARG1* coding sequences counteracts the influence of increased SAGA occupancy. Indeed, it was shown recently that transcription coupled methylation of H3-K36 by Set2p stimulates recruitment of the Rpd3p "small" (Rpd3-S) complex to coding sequences dependent on the Eaf3p subunit (Carrozza et al., 2005; Joshi and Struhl, 2005; Keogh et al., 2005). At odds with this possibility, no increase in the H3Ac/H3 ratio in *eaf3Δ* or *set2Δ* mutants was seen (Figure 6E). The same was true for mutants with single deletions of *RPD3* or the HDAs encoded by *HOS1*, *HOS2*, and *HOS3* (Figure S3 and data not shown). However, in a *hos2Δ hos3Δ rpd3Δ* triple mutant, we saw substantially higher H3 acetylation per nucleosome at 5′ ORF and 3′ ORF sequences and moderately greater acetylation of UAS and TATA nucleosomes (Figure 6H), all without a significant change in total H3 levels (Figure 6G). These findings suggest that induction by Gcn4p increases the rate of H3 deacetylation by several HDAs, which offsets the increased acetylation afforded by SAGA association with the coding region. Consistent with this model, we observed recruitment of Rpd3p and Hos2p to *ARG1* during induction by Gcn4p, with highest occupancies at the 3′ end of the ORF (Figure 6I).

Gcn5p Promotes H3-K4 Methylation

There is evidence that SAGA component Ubp8p promotes H3-K4 trimethylation (H3-K4me3) in the 5′ ends of coding regions (Daniel et al., 2004). Chd1p, also associated with SAGA (Pray-Grant et al., 2005), interacts with Rtf1p and Spt4p/Spt5p complex (Simic et al., 2003), which in turn stimulate H3-K4 trimethylation (Qiu et al., 2006; Sims et al., 2004). Thus, it was possible that association of SAGA with the coding region promotes H3-K4 methylation in the ORF. Supporting this idea, *gcn5Δ* cells show reduced levels of H3-K4me3 in bulk histones, although not to the same extent observed in *bre1Δ* cells lacking H2B ubiquitination activity (Figure 7A). ChIP analysis of the *ARG1* gene reveals a Gcn4p-dependent increase in H3-K4me3 per nucleosome in 5′ ORF sequences that is reduced by *gcn5Δ* (Figure 7B). Thus, it appears that H3 acetylation by Gcn5p promotes trimethylation of H3-K4 in the *ARG1* coding region during transcriptional induction by Gcn4p.

DISCUSSION

We have shown that SAGA is associated with coding regions of *GAL1* and Gcn4p target genes under inducing conditions and demonstrated a role for Gcn5p and SAGA in transcription-coupled histone modifications and nucleosome eviction in ORF sequences. The presence of SAGA in the coding sequences of induced *ARG1* requires PIC assembly and transcription (being impaired by deletion of the TATA element) and is stimulated by Ser5-CTD phosphorylation by Kin28p. Thus, SAGA could migrate from the UAS to the ORF by binding to the Ser5-phosphorylated CTD or another CTD-binding factor. Alternatively, SAGA could recognize a nucleosome modification that requires Ser5-CTD phosphorylation other than H2B ubiquitination (Xiao et al., 2005) and H3-K4 trimethylation (Ng et al., 2003), which we excluded as requirements for SAGA association with the ORF.

Genome-wide analysis of transcription in rich glucose (YPD) medium revealed association of SAGA with coding sequences, but much higher SAGA occupancies in the UAS elements (Robert et al., 2004). By contrast, we observed comparable levels of SAGA in UAS and ORF regions of induced *GAL1* and *ARG1*. To explain this inconsistency, we note that neither Gcn4p nor Gal4p functions efficiently in YPD, so their roles in SAGA recruitment were excluded in the genome-wide study. It was also shown that SAGA is restricted to the UAS at *GAL1* under inducing conditions (Larschan and Winston, 2001). To account for this discrepancy, we suggest that SAGA association is labile and more dependent on the exact crosslinking conditions and strain background than is SAGA association with activators at UAS elements.

We obtained evidence that SAGA mediates transcription-coupled acetylation of ORF nucleosomes by Gcn5p. During induction of *GAL1*, coding regions as well as promoters undergo increased H3 acetylation per nucleosome by Gcn5p during transcriptional activation. The fact that disruption of SAGA but not ADA reduced the H3Ac/H3 ratio in the *GAL1* ORF suggests that Gcn5p acts in SAGA, not ADA, to acetylate H3 during transcriptional induction. However, because disruption of SAGA impairs transcription, and acetylation of ORF nucleosomes requires transcription, an unknown Gcn5p complex that would also associate with transcribed coding regions could mediate H3 acetylation in the ORF during induction.

Our results differ from previous reports of a strong increase (Krebs et al., 2000) or no change (Deckert and Struhl, 2001; Topalidou et al., 2003) in absolute levels of H3Ac in the induced *GAL1* promoter, as we observed a decline in H3Ac at the UAS. However, because total H3 levels were not analyzed in the previous studies, the H3Ac/H3 ratios cannot be assessed. No change in H3Ac per nucleosome was observed in the *GAL10-VPS13* ORF (Kristjuhan and Svejstrup, 2004), in contrast to the increase observed here for authentic *GAL1*. Perhaps a histone deacetylase is more active in the *GAL10-VPS13* ORF compared to authentic *GAL1*.

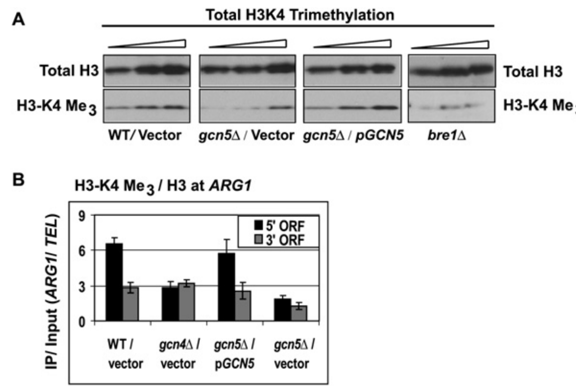

Figure 7. Gcn5p Promotes H3-K4 Trimethylation In Vivo

(A) *GCN5* strain HQY392 bearing empty vector and *gcn5Δ* strain CGY99 with vector or *GCN5* plasmid p316-GCN5 were grown in SC-Ura, whereas *bre1Δ* strain CGY57 was grown in YPD, and WCEs were subjected to western analysis with antibodies against total histone H3 or H3-K4Me$_3$. The panels derive from the same western blots.
(B) ChIP analysis of total H3 and H3-K4Me$_3$ at *ARG1* in the same strains as in (A) in cultures induced for Gcn4p synthesis by SM. The ratio of H3-K4Me3 to total H3 occupancy is plotted for the indicated strains. All error bars represent the SEM.

Turning to *ARG1*, despite an increased H3Ac/H3 ratio in the promoter on induction by Gcn4p, we saw no change in, or even reduced amounts of, H3Ac/H3 in the ORF. Compared to *GAL1*, only a small reduction in nucleosome density in the ORF was observed, probably reflecting a lower transcription rate for *ARG1*. The decreased acetylation of ORF nucleosomes was transcription dependent since disruption of SAGA (*ada1Δ*) or deletion of the TATA element led to a higher H3Ac/H3 ratio in the ORF and lower H3Ac/H3 in the promoter, and both trends reflect the basal acetylation state of uninduced *ARG1*. Thus, while Gcn5p is responsible for the bulk of H3Ac in the *ARG1* ORF, SAGA occupancy of the ORF does not yield the expected increase in H3 acetylation compared to that seen in noninducing conditions.

The resolution of this last paradox seems to be that induction of *ARG1* elicits increased deacetylation of H3 by multiple HDAs to an extent that offsets elevated Gcn5p occupancy in the ORF. A triple mutant lacking the HDAs Hos2p, Hos3p, and Rpd3p shows increased H3Ac per nucleosome in the ORF and promoter regions, whereas single deletions of these HDAs had little effect on H3 acetylation at *ARG1*. Thus, it appears that Hos2p, Hos3p, and Rpd3p have overlapping functions in H3 deacetylation at *ARG1*. Our finding that deletion of the *ARG1* TATA increases the H3Ac/H3 ratio in the ORF (Figure 6E) further suggests that ORF-occupancy of HDAs is coupled to transcription of *ARG1*, which we confirmed by ChIP analysis of Rpd3p and Hos2p (Figure 6I). Previous studies showed that Hos2p but not Rpd3p is recruited to the coding sequences of induced *GAL* genes (Wang et al., 2002).

Thus, to explain our findings on H3 acetylation at *ARG1*, we propose that induction by Gcn4p leads to increased rates of acetylation by SAGA and deacetylation by multiple HDAs to yield unchanged or decreased H3Ac in the ORF but increased H3Ac in the promoter. The different outcomes for ORF and promoter are likely explained by greater recruitment of HDAs to the ORF versus promoter. At *GAL1*, the balance between acetylation and deacetylation differs so that transcriptional induction elicits higher H3Ac per nucleosome in both ORF and promoter sequences. Our results are reminiscent of previous findings that transcriptional induction limits H3 acetylation in the promoters of various yeast genes and that Rpd3p is involved in reversing acetylation of promoter histones at *PHO5* (Topalidou et al., 2003). Our observations extend this principle to include nucleosomes in the coding regions of Gcn4p-induced genes and demonstrate that Hos2p or Hos3p, in addition to Rpd3p, promote deacetylation of ORF nucleosomes. The balance between SAGA and HDAs may establish the proper level of histone acetylation in the ORF needed to maximize transcription, or transcription-coupled events, while avoiding the deleterious effects of hyperacetylation in activating cryptic internal promoters (Carrozza et al., 2005; Joshi and Struhl, 2005).

We obtained evidence that hypoacetylation of ORF nucleosomes in *gcn5Δ* cells reduces nucleosome eviction from the *GAL1* and P_{GAL}-*YLR454* ORFs during galactose induction. Acetylation of H3 by Gcn5p may weaken nucleosome-DNA or internucleosomal interactions (Spencer and Davie, 1999) as a way of enhancing nucleosome eviction. The histone chaperone Asf1p is the only other factor implicated in transcription-coupled histone eviction from coding sequences in vivo. Like Gcn5p, Asf1p promotes but is not essential for histone eviction from the ORF at Gal4p-induced genes (Schwabish and Struhl, 2006). It is noteworthy that *ada1Δ* but not *gcn5Δ* diminished histone loss from the induced *GAL1* promoter. Thus, both HAT and non-HAT functions of SAGA contribute to histone eviction at different locations at *GAL1*.

The diminished nucleosome eviction in the P_{GAL}-*YLR454* ORF in *gcn5Δ* cells is accompanied by decreased Pol II occupancy at the 3′ end of the ORF, consistent with reduced processivity. That lower Pol II occupancy was not observed for *GAL1* is consistent with its smaller length (~1.6 kb) and the fact that Pol II occupancy is affected at P_{GAL1}-*YLR454* only at distances ≥4 kb from the promoter. Interestingly, *gcn5Δ* reduced mRNA production significantly more from P_{GAL1}-*YLR454* than from *GAL1*, and as P_{GAL1}-*YLR454* and *GAL1* have the same promoter, this difference implies an elongation defect. We propose that less efficient nucleosome eviction impairs Pol II processivity and results in reduced transcript production from the long P_{GAL1}-*YLR454* ORF much more than from the shorter *GAL1* gene. The average ORF length of genes dependent on Gcn5p for maximum transcription in YPD (Holstege et al., 1998) is not significantly larger than the average ORF length for the entire genome; however, many shorter genes may require Gcn5p for PIC assembly or promoter clearance rather than elongation, making it difficult to determine whether Gcn5p is generally required for optimal elongation through long ORFs. However, supporting our conclusion, it was shown recently that *gcn5Δ* and *spt3Δ* reduce mRNA expression in yeast cells from long (4.5 kb) but not short (1.5 kb) transcription units placed under the control of the same (*GAL1*) promoter (Morillo-Huesca et al., 2006).

Interestingly, we found that H3 acetylation increases with kinetics indistinguishable from that of nucleosome reassembly following run-off of Pol II molecules from the P_{GAL1}-*YLR454* ORF on glucose repression. It was shown previously that the dissociation of HDAs that were reversibly tethered to a yeast promoter is accompanied by reacetylation of nucleosomes within 5–8 min (Katan-Khaykovich and Struhl, 2002). We observed recovery of acetylated nucleosomes within 1 min of the passage of Pol II in the P_{GAL1}-*YLR454* ORF. Hence, the presence of SAGA in the ORF may ensure instantaneous acetylation of reassembled nucleosomes in the wake of elongating Pol II. This could explain why the level of acetylated H3 per nucleosome is higher immediately following glucose repression (when SAGA may still persist in the ORF) than under noninducing conditions (when SAGA is absent) (Figure 4D, lanes 1 and 3). Rapid acetylation of reassembled nucleosomes may help prevent formation of silenced chromatin domains at inducible genes, as heterochromatin formation is antagonized by Gcn5p (Ishii and Laemmli, 2003; Oki et al., 2004).

EXPERIMENTAL PROCEDURES

Yeast strains employed are listed in Table S1 and described in the Supplemental Data, along with the antibodies and PCR primers employed (Table S2). Plasmids pRS316-GCN5 (Marcus et al., 1994) and pGAL1-YLR454 (Mason and Struhl, 2005) were described previously. SC and YP medium were prepared as described (Sherman et al., 1974), and ChIP was conducted as described in the Supplemental Data. Whole-cell extracts were prepared by trichloroacetic acid precipitation (Reid and Schatz, 1982), and western analysis was conducted as described (Zhang et al., 2004). Northern blotting was performed as described previously (Swanson et al., 2003).

Supplemental Data

Supplemental Data include two tables, four figures, Supplemental Experimental Procedures, and References and can be found with this article online at http://www.molecule.org/cgi/content/full/25/1/31/DC1/.

ACKNOWLEDGMENTS

We thank Steve Hahn, Kevan Shokat, Mark Solomon, Kevin Struhl, David Stillman, Mike Hampsey, Lenny Guarente, Mark Ptashne, and Joe Reese for gifts of strains, plasmids, or antibodies, and Fred Winston and Steve Buratowski for critical reading of the manuscript. This research was supported in part by the Intramural Research Program of the NIH, NICHD.

Received: June 19, 2006
Revised: October 7, 2006
Accepted: November 22, 2006
Published: January 11, 2007

REFERENCES

Ansari, A., and Hampsey, M. (2005). A role for the CPF 3'-end processing machinery in RNAP II-dependent gene looping. Genes Dev. *19*, 2969–2978.

Barbaric, S., Walker, J., Schmid, A., Svejstrup, J.Q., and Horz, W. (2001). Increasing the rate of chromatin remodeling and gene activation–a novel role for the histone acetyltransferase Gcn5. EMBO J. *20*, 4944–4951.

Bhaumik, S.R., and Green, M.R. (2001). SAGA is an essential in vivo target of the yeast acidic activator Gal4p. Genes Dev. *15*, 1935–1945.

Bhaumik, S.R., and Green, M.R. (2002). Differential requirement of SAGA components for recruitment of TATA-box- binding protein to promoters in vivo. Mol. Cell. Biol. *22*, 7365–7371.

Carrozza, M.J., Li, B., Florens, L., Suganuma, T., Swanson, S.K., Lee, K.K., Shia, W.J., Anderson, S., Yates, J., Washburn, M.P., and Workman, J.L. (2005). Histone H3 methylation by Set2 directs deacetylation of coding regions by Rpd3S to suppress spurious intragenic transcription. Cell *123*, 581–592.

Cosma, M.P., Tanaka, T., and Nasmyth, K. (1999). Ordered recruitment of transcription and chromatin remodeling factors to a cell cycle- and developmentally regulated promoter. Cell *97*, 299–311.

Daniel, J.A., Torok, M.S., Sun, Z.W., Schieltz, D., Allis, C.D., Yates, J.R., 3rd, and Grant, P.A. (2004). Deubiquitination of histone H2B by a yeast acetyltransferase complex regulates transcription. J. Biol. Chem. *279*, 1867–1871.

Deckert, J., and Struhl, K. (2001). Histone acetylation at promoters is differentially affected by specific activators and repressors. Mol. Cell. Biol. *21*, 2726–2735.

Dudley, A.M., Rougeulle, C., and Winston, F. (1999). The Spt components of SAGA facilitate TBP binding to a promoter at a post-activator-binding step in vivo. Genes Dev. *13*, 2940–2945.

Eberharter, A., Sterner, D.E., Schieltz, D., Hassan, A., Yates, J.R., Berger, S.L., and Workman, J.L. (1999). The ADA Complex Is a Distinct Histone Acetyltransferase Complex in *Saccharomyces cerevisiae*. Mol. Cell. Biol. *19*, 6621–6631.

Filetici, P., Aranda, C., Gonzalez, A., and Ballario, P. (1998). GCN5, a yeast transcriptional coactivator, induces chromatin reconfiguration of HIS3 promoter in vivo. Biochem. Biophys. Res. Commun. *242*, 84–87.

Geng, F., and Laurent, B.C. (2004). Roles of SWI/SNF and HATs throughout the dynamic transcription of a yeast glucose-repressible gene. EMBO J. *23*, 127–137.

Govind, C.K., Yoon, S., Qiu, H., Govind, S., and Hinnebusch, A.G. (2005). Simultaneous Recruitment of Coactivators by Gcn4p Stimulates Multiple Steps of Transcription in vivo. Mol. Cell. Biol. *25*, 5626–5638.

Holstege, F.C., Jennings, E.G., Wyrick, J.J., Lee, T.I., Hengartner, C.J., Green, M.R., Golub, T.R., Lander, E.S., and Young, R.A. (1998). Dissecting the regulatory circuitry of a eukaryotic genome. Cell *95*, 717–728.

Ishii, K., and Laemmli, U.K. (2003). Structural and dynamic functions establish chromatin domains. Mol. Cell *11*, 237–248.

Joshi, A.A., and Struhl, K. (2005). Eaf3 chromodomain interaction with methylated H3-K36 links histone deacetylation to Pol II elongation. Mol. Cell *20*, 971–978.

Katan-Khaykovich, Y., and Struhl, K. (2002). Dynamics of global histone acetylation and deacetylation in vivo: rapid restoration of normal histone acetylation status upon removal of activators and repressors. Genes Dev. *16*, 743–752.

Keogh, M.C., Kurdistani, S.K., Morris, S.A., Ahn, S.H., Podolny, V., Collins, S.R., Schuldiner, M., Chin, K., Punna, T., Thompson, N.J., et al. (2005). Cotranscriptional set2 methylation of histone H3 lysine 36 recruits a repressive Rpd3 complex. Cell *123*, 593–605.

Krebs, J.E., Fry, C.J., Samuels, M.L., and Peterson, C.L. (2000). Global Role for Chromatin Remodeling Enzymes in Mitotic Gene Expression. Cell *102*, 587–598.

Krebs, J.E., Kuo, M.H., Allis, C.D., and Peterson, C.L. (1999). Cell cycle-regulated histone acetylation required for expression of the yeast *HO* gene. Genes Dev. *13*, 1412–1421.

Krishnamurthy, S., He, X., Reyes-Reyes, M., Moore, C., and Hampsey, M. (2004). Ssu72 Is an RNA polymerase II CTD phosphatase. Mol. Cell *14*, 387–394.

Kristjuhan, A., and Svejstrup, J.Q. (2004). Evidence for distinct mechanisms facilitating transcript elongation through chromatin in vivo. EMBO J. *23*, 4243–4252.

Kristjuhan, A., Walker, J., Suka, N., Grunstein, M., Roberts, D., Cairns, B.R., and Svejstrup, J.Q. (2002). Transcriptional inhibition of genes with severe histone h3 hypoacetylation in the coding region. Mol. Cell *10*, 925–933.

Kuo, M.H., vom Bauer, E., Struhl, K., and Allis, C.D. (2000). Gcn4 activator targets Gcn5 histone acetyltransferase to specific promoters Independently of transcription. Mol. Cell *6*, 1309–1320.

Larschan, E., and Winston, F. (2001). The *S. cerevisiae* SAGA complex functions in vivo as a coactivator for transcriptional activation by Gal4. Genes Dev. *15*, 1946–1956.

Linger, J., and Tyler, J.K. (2006). Global replication-independent histone h4 exchange in budding yeast. Eukaryot. Cell *5*, 1780–1787.

Marcus, G.A., Silverman, N., Berger, S.L., Horiuchi, J., and Guarente, L. (1994). Functional similarity and physical association between GCN5 and ADA2: putative transcriptional adaptors. EMBO J. *13*, 4807–4815.

Mason, P.B., and Struhl, K. (2005). Distinction and relationship between elongation rate and processivity of RNA polymerase II in vivo. Mol. Cell *17*, 831–840.

Milgrom, E., West, R.W., Jr., Gao, C., and Shen, W.C. (2005). TFIID and Spt-Ada-Gcn5-acetyltransferase functions probed by genome-wide synthetic genetic array analysis using a Saccharomyces cerevisiae taf9-ts allele. Genetics *171*, 959–973.

Morillo-Huesca, M., Vanti, M., and Chavez, S. (2006). A simple in vivo assay for measuring the efficiency of gene length-dependent processes in yeast mRNA biogenesis. FEBS J. *273*, 756–769.

Ng, H.H., Robert, F., Young, R.A., and Struhl, K. (2003). Targeted recruitment of Set1 histone methylase by elongating Pol II provides a localized mark and memory of recent transcriptional activity. Mol. Cell *11*, 709–719.

Oki, M., Valenzuela, L., Chiba, T., Ito, T., and Kamakaka, R.T. (2004). Barrier proteins remodel and modify chromatin to restrict silenced domains. Mol. Cell. Biol. *24*, 1956–1967.

O'Sullivan, J.M., Tan-Wong, S.M., Morillon, A., Lee, B., Coles, J., Mellor, J., and Proudfoot, N.J. (2004). Gene loops juxtapose promoters and terminators in yeast. Nat. Genet. *36*, 1014–1018.

Pray-Grant, M.G., Daniel, J.A., Schieltz, D., Yates, J.R., 3rd, and Grant, P.A. (2005). Chd1 chromodomain links histone H3 methylation with SAGA- and SLIK-dependent acetylation. Nature *433*, 434–438.

Qiu, H., Hu, C., Wong, C.M., and Hinnebusch, A.G. (2006). The Spt4p Subunit of Yeast DSIF Stimulates Association of the Paf1 Complex with Elongating RNA Polymerase II. Mol. Cell. Biol. *26*, 3135–3148.

Qiu, H., Hu, C., Yoon, S., Natarajan, K., Swanson, M., and Hinnebusch, A.G. (2004). An array of coactivators is required for optimal recruitment of TBP and RNA Polymerase II by promoter-bound Gcn4p. Mol. Cell. Biol. *24*, 4104–4117.

Qiu, H., Hu, C., Zhang, F., Hwang, G., Swanson, M., Boonchird, C., and Hinnebusch, A.G. (2005). Interdependent recruitment of SAGA and Srb mediator by transcriptional activator Gcn4p. Mol. Cell. Biol. *25*, 3461–3474.

Reid, G.A., and Schatz, G. (1982). Import of Proteins into Mitochondria. J. Biol. Chem. *257*, 13062–13067.

Reinke, H., and Horz, W. (2003). Histones are first hyperacetylated and then lose contact with the activated PHO5 promoter. Mol. Cell *11*, 1599–1607.

Robert, F., Pokholok, D.K., Hannett, N.M., Rinaldi, N.J., Chandy, M., Rolfe, A., Workman, J.L., Gifford, D.K., and Young, R.A. (2004). Global position and recruitment of HATs and HDACs in the yeast genome. Mol. Cell *16*, 199–209.

Schermer, U.J., Korber, P., and Horz, W. (2005). Histones are incorporated in trans during reassembly of the yeast PHO5 promoter. Mol. Cell *19*, 279–285.

Schwabish, M.A., and Struhl, K. (2004). Evidence for eviction and rapid deposition of histones upon transcriptional elongation by RNA polymerase II. Mol. Cell. Biol. *24*, 10111–10117.

Schwabish, M.A., and Struhl, K. (2006). Asf1 mediates histone eviction and deposition during elongation by RNA polymerase II. Mol. Cell *22*, 415–422.

Sherman, F., Fink, G.R., and Lawrence, C.W. (1974). Methods of Yeast Genetics (Cold Spring Harbor, NY: Cold Spring Harbor Laboratory Press).

Simic, R., Lindstrom, D.L., Tran, H.G., Roinick, K.L., Costa, P.J., Johnson, A.D., Hartzog, G.A., and Arndt, K.M. (2003). Chromatin remodeling protein Chd1 interacts with transcription elongation factors and localizes to transcribed genes. EMBO J. *22*, 1846–1856.

Sims, R.J., 3rd, Belotserkovskaya, R., and Reinberg, D. (2004). Elongation by RNA polymerase II: the short and long of it. Genes Dev. *18*, 2437–2468.

Spencer, V.A., and Davie, J.R. (1999). Role of covalent modificaitons of histones in regulating gene expression. Gene *240*, 1–12.

Swanson, M.J., Qiu, H., Sumibcay, L., Krueger, A., Kim, S.-J., Natarajan, K., Yoon, S., and Hinnebusch, A.G. (2003). A Multiplicity of coactivators is required by Gcn4p at individual promoters in vivo. Mol. Cell. Biol. *23*, 2800–2820.

Topalidou, I., Papamichos-Chronakis, M., and Thireos, G. (2003). Post-TATA binding protein recruitment clearance of Gcn5-dependent histone acetylation within promoter nucleosomes. Mol. Cell. Biol. *23*, 7809–7817.

Vogelauer, M., Wu, J., Suka, N., and Grunstein, M. (2000). Global histone acetylation and deacetylation in yeast. Nature *408*, 495–498.

Wang, A., Kurdistani, S.K., and Grunstein, M. (2002). Requirement of Hos2 histone deacetylase for gene activity in yeast. Science *298*, 1412–1414.

Wery, M., Shematorova, E., Van Driessche, B., Vandenhaute, J., Thuriaux, P., and Van Mullem, V. (2004). Members of the SAGA and Mediator complexes are partners of the transcription elongation factor TFIIS. EMBO J. *23*, 4232–4242.

Xiao, T., Kao, C.F., Krogan, N.J., Sun, Z.W., Greenblatt, J.F., Osley, M.A., and Strahl, B.D. (2005). Histone H2B ubiquitylation is associated with elongating RNA polymerase II. Mol. Cell. Biol. *25*, 637–651.

Zhang, F., Sumibcay, L., Hinnebusch, A.G., and Swanson, M.J. (2004). A triad of subunits from the Gal11/tail domain of Srb mediator is an in vivo target of transcriptional activator Gcn4p. Mol. Cell. Biol. *24*, 6871–6886.

Zhang, Z., and Reese, J.C. (2004). Ssn6-Tup1 requires the ISW2 complex to position nucleosomes in Saccharomyces cerevisiae. EMBO J. *23*, 2246–2257.